J Chem Crystallogr (2012) 42:752–758
DOI 10.1007/s10870-012-0312-y

ORIGINAL PAPER

Extensive Intramolecular and Intermolecular Interactions in Two Quaternary Salts of the Pyridoxal Oxime

Mario Cetina · Ante Nagl · Dajana Gašo-Sokač · Spomenka Kovač · Valentina Bušić · Dijana Saftić

Received: 8 November 2011 / Accepted: 31 March 2012 / Published online: 27 April 2012

Abstract Two derivatives of pyridoxal oxime (**1**) were prepared by quaternization of pyridoxal oxime with phenacyl bromide and 2-methoxyphenacyl bromide. The crystal structures of the 1-phenacyl-3-hydroxy-4-hydroxyiminomethyl-5-hydroxymethyl-2-methylpyridinium bromide (**2**) and the novel 3-hydroxy-4-hydroxyiminomethyl-5-hydroxymethyl-2-methyl-1-(2′-methoxyphenacyl) pyridinium bromide (**3**) have been determined by X-ray diffraction method. The conformation of these two pyridoxal oxime phenacyl derivatives is locked by numerous intramolecular hydrogen bonds. The O–H···Br, C–H···Br and C–H···O hydrogen bonds in **2** and **3** form complex three-dimensional network. Supramolecular structure of **3** also contains C–H···π and π···π interactions which link neighbouring cations.

Keywords Quaternary pyridinium salts · Phenacyl bromides · Pyridoxal oxime derivatives · X-ray diffraction · Supramolecular assembling

M. Cetina (✉) · A. Nagl
Department of Applied Chemistry, Faculty of Textile Technology, University of Zagreb, Prilaz baruna Filipovića 28a, 10000 Zagreb, Croatia
e-mail: mario.cetina@ttf.hr

D. Gašo-Sokač · S. Kovač · V. Bušić
Department of Chemistry, J.J. Strossmayer University of Osijek, Kuhačeva 20, 31000 Osijek, Croatia

D. Gašo-Sokač (✉) · S. Kovač
Faculty of Food Technology, J.J. Strossmayer University of Osijek, Kuhačeva 20, 31000 Osijek, Croatia
e-mail: dajana.gaso@ptfos.hr

D. Saftić
Ruđer Bošković Institute, Bijenička 54, 10000 Zagreb, Croatia

Introduction

The organophosphorus compounds are widely used in agriculture as insecticides, in industry and technology, as well as in military technology as chemical warfare agents (sarin, soman, tabun). They are extremely potent inhibitors of the enzyme acetylcholinesterase (AChE) that is responsible for the termination of the action of acetylcholine at cholinergic synapses [1, 2]. There are many commonly used reactivators of inhibited AChE, such as 2-pralidoxime, trimedoxime and toxogonin [3–6]. Unfortunately, none of the currently used oximes is sufficiently effective against all inhibitors and there is no single reactivator having the ability to reactivate inhibited enzyme regardless of the chemical structure of the inhibitor [7, 8]. Commonly used reactivators are characterised by the presence of several structural features: functional oxime group, quaternary nitrogen atom and different length of linking chain between two pyridinium rings in the case of bispyridinium reactivators [9, 10]. Pyridoxal oxime, a derivative of B_6 vitamin, meets some of these structural features and can be used for synthesis of compounds structurally similar to common antidotes. Milatović et al. [11] synthesized three new dioximes which combine the structure features of pyridoxal oxime and toxogonine. Gašo-Sokač et. al. [12] synthesized a series of novel pyridinium oximes and tested them as reactivators of AChE inhibited by organophosphorus compounds tabun and paraoxon.

In this paper, we report the structures of two pyridoxal oximes, 1-phenacyl-3-hydroxy-4-hydroxyiminomethyl-5-hydroxymethyl-2-methyl pyridinium bromide (**2**) [12] and 3-hydroxy-4-hydroxyiminomethyl-5-hydroxymethyl-2-methyl-1-(2′-methoxyphenacyl) pyridinium bromide (**3**). Pyridoxal oxime quaternary salts were prepared by quaternization

of the pyridoxal oxime (**1**) with phenacyl bromide and 2-methoxylphenacyl bromide (Scheme 1). In this work we particularly pay attention on supramolecular assembling of these two compounds as bromides and cations, which possess three hydroxyl groups, can form an intricate network of hydrogen bonds.

Experimental Section

Solvents and reagents were purchased from Fluka and Aldrich and used without further purification. IR spectra were measured on Paragon 500 FT-IR spectrophotometer with KBr pellets. ^{1}H NMR and ^{13}C NMR spectra were measured on a Varian XL-GEM 300 spectrophotometer in DMSO-d_6 solutions and chemical shifts are reported in δ values downfield from TMS as an internal standard. Melting points were determined with capillary melting point apparatus Stuart melting point apparatus SMP3. The purity of compound was determined by ^{1}H NMR, ^{13}C NMR and elemental analysis. The single crystals were obtained at room temperature by slow evaporation of a methanol solution.

Synthesis

Synthesis of 1-phenacyl-3-hydroxy-4-hydroxyiminomethyl-5-hydroxymethyl-2-methyl pyridinium bromide (**2**) has been described previously [12].

*Synthesis of 3-hydroxy-4-hydroxyiminomethyl-5-hydroxymethyl-2-methyl-1-(2′-methoxyphenacyl) pyridinium bromide (**3**)*

Pyridoxal oxime (**1**) (0.36 g; 2 mmol) was dissolved in acetone (300 mL) and stirred 20 min at 50 °C. The reaction mixture was cooled to room temperature, and 2-methoxyphenacyl bromide was added (0.46 g; 2 mmol). The reaction mixture was stirred for 24 h at room temperature, and left in dark for 3 weeks. The crystalline crude product was collected by filtration under reduce pressure and recrystallized from methanol.

Brown solid, mp: 217–219 °C. Yield: 12 %. IR (KBr, cm^{-1}): 3309, 3103–2935, 1676, 1597–1437, 1254, 1049–979. ^{1}H NMR (DMSO-d_6) δ 13.03 (bs, 1H, NO*H*); 11.90 (bs, 1H, O*H*); 8.66 (s, 1H, H-6); 8.62 (s, 1H, H-3″); 7.85 (d, 1H, H-5″); 7.74 (d, 1H, H-6″); 7.35 (d, 1H, H-4″); 7.15 (s, 2H,CH_2CO); 6.28 (bs, 1H, CH_2OH). ^{13}C NMR (DMSO-d_6) δ 189.89 (CO); 152.54 (C-3); 145.56 (C-4′); 145.51 (C-2); 139.71 (C-4); 137.35 (C-6); 135.11 (C-1″); 132.28 (C-2″, C-6″); 130.50 (C-3″, C-5″); 128.18 (C-5); 64.52 [CH_2(C-5′)]; 58.53 (CH_2CO′); 13.37 [(CH_3 (C-2′)]. Elemental analysis for $C_{17}H_{19}N_2O_5Br$: Found (Calculated): C 49.60 (49.65), H 4.65 (4.66), N 6.58 (6.81) %.

X-ray Crystal Structure Determination

The intensities were collected at 295 K on a Oxford diffraction Xcalibur2 diffractometer with a Sapphire 3 CCD detector using graphite-monochromated MoK_α radiation ($\lambda = 0.71073$ Å). The data collection and reduction were carried out with the *CrysAlis* programs [13]. The intensities were corrected for absorption using the multi-scan absorption correction method by *CrysAlis RED* [13]. Details of crystal data, data collection and refinement parameters are given in Table 1. The crystal structures were solved by direct methods [14]. All non-hydrogen atoms were refined anisotropically by full-matrix least-squares calculations based on F^2 [14]. The hydrogen atoms attached to the O1 and O2 atoms in **2**, as well as O1A, O2A, O3A, O1B and O2B in **3** were found in a difference Fourier map and their coordinates and isotropic thermal parameters have been refined freely. All other hydrogen atoms were treated using appropriate riding models, with *SHELXL97* defaults [14]. *PLATON* program was used for analysis and molecular and crystal structure drawings preparation [15]. CCDC 756361 and 756362 contain the supplementary crystallographic data for this paper. These data can be obtained free of charge from The Cambridge Crystallographic Data Centre via www.ccdc.cam.ac.uk/data_request/cif.

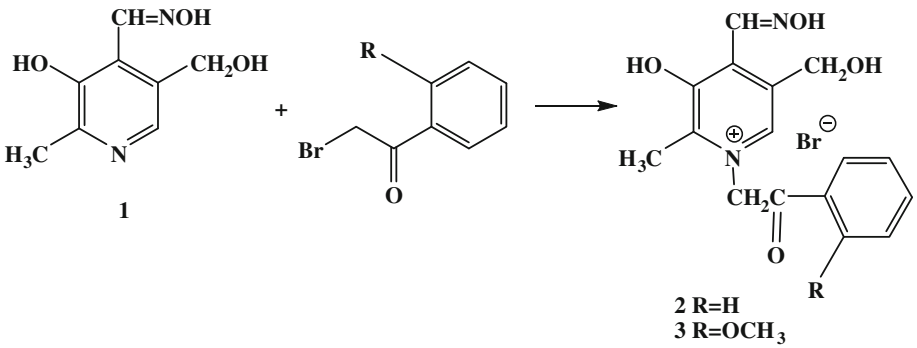

Scheme 1 Synthesis of the oximes **2** and **3**

Table 1 X-ray crystallographic data for **2** and **3**

Compound	**2**	**3**
Formula	$C_{16}H_{17}BrN_2O_4$	$C_{17}H_{19}BrN_2O_5$
Formula weight	381.23	411.25
Crystal size [mm]	0.10 × 0.33 × 0.40	0.22 × 0.45 × 0.49
Crystal colour, shape	Yellow, prism	Yellow, irregular
Crystal system	Monoclinic	Triclinic
Space group	$P\ 2_1/c$	$P\bar{1}$
Unit cell dimensions		
a [Å]	9.3672 (3)	8.6597 (2)
b [Å]	11.1758 (3)	14.4279 (4)
c [Å]	16.6843 (6)	15.4781 (4)
α [°]	90	70.202 (3)
β [°]	111.097 (3)	78.376 (2)
γ [°]	90	86.411 (2)
V [Å^3]	1629.54 (9)	1782.20 (8)
Z	4	4
$D_{calc.}$ [g cm^{-3}]	1.554	1.533
Absorption coefficient μ [mm^{-1}]	2.544	2.336
Scan mode	ω scans	ω scans
θ range [°]	3.87–27.99	3.90–28.00
Index ranges	$-12 \le h \le 12$	$-11 \le h \le 11$
	$-14 \le k \le 14$	$-19 \le k \le 19$
	$-21 \le l \le 22$	$-20 \le l \le 20$
Collected reflections no.	20,541	41,626
Independent reflections no./$R_{int.}$	3924/0.0387	8588/0.0322
Reflections no. $I \ge 2\sigma(I)$	2,464	4,566
Data/parameters ratio	3924/218	8588/487
Transmission factors, T_{min}/T_{max}	0.62687/1.0000	0.80803/1.0000
Goodness-of-fit on F^2, S	0.989	0.902
R [$I \ge 2\sigma(I)$]/R [all data]	0.0325/0.0580	0.0333/0.0780
wR [$I \ge 2\sigma(I)$]/wR [all data]	0.0767/0.0795	0.0733/0.0777
Max./min. electron density [e Å^{-3}]	0.554/−0.677	0.723/−0.440

Results and Discussion

Compound **2** crystallizes in monoclinic space group $P\ 2_1/c$ (Fig. 1), while compound **3** crystallizes in triclinic space group $P\bar{1}$ with two independent cations, denoted as A and B (Fig. 2), and two bromides in the asymmetric unit. The O3B atom in B cation of compound **3** is disordered over two sites, with the occupancies refined to 0.691(5) and 0.309(5), respectively. The geometrical parameters of **2**

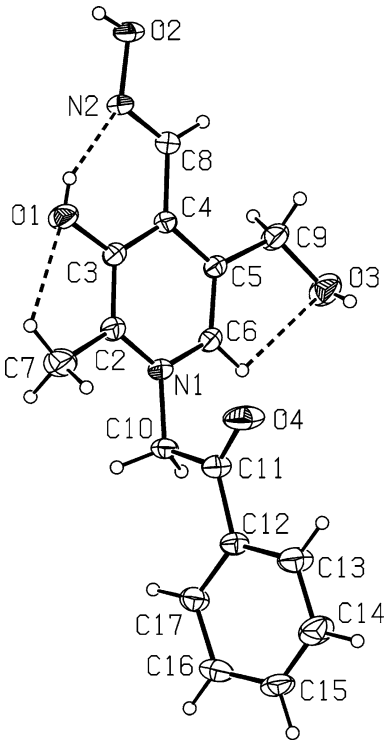

Fig. 1 A molecular structure of cation of **2**, with the atom-numbering scheme. Displacement ellipsoids for nonhydrogen atoms are drawn at the 30 % probability level. Intramolecular hydrogen bonds are shown dashed

and **3** are very close to already published similar structures, 3-hydroxy-4-hydroxyiminomethyl-5-hydroxymethyl-1,2-dimethylpyridinium iodide and 3-hydroxy-4-hydroxyiminomethyl-5-hydroxymethyl-1,2-dimethylpyridinium chloride monohydrate [16]. A survey of Cambridge structural database [17] revealed that above mentioned structures are the only two 4-(hydroxyiminomethyl) pyridinium derivatives which have bonded methyl group to C-2 atom, hydroxyl group to C-3 and hydroxymethyl group to C-5 atom of the pyridinium ring.

In both structures, one intramolecular hydrogen bond of O–H···N type, O1···N2, forms $S(6)$ [18] ring (Table 2). Furthermore, the C7···O1 intramolecular hydrogen bond generates five-membered ring of $S(5)$ type. There are lot of other intramolecular hydrogen bonds that lock conformation of **2** and **3** through five-membered and six-membered rings. Orientation of the hydroxymethyl group with respect to the pyridinium ring represents the first conformational difference between **2** and **3** and between two independent cations of **3**. The conformation defined by torsion angle C6–C5–C9–O3 is *synperiplanar* in **2** [−8.7(3)°] and A cation of **3** [–3.4(3)°]. Such conformation enables C6···O3 intramolecular hydrogen bond formation. On the contrary, major component of the hydroxyl oxygen atom O3 in B cation of **3** is in *anticlinal* disposition towards C6 atom of

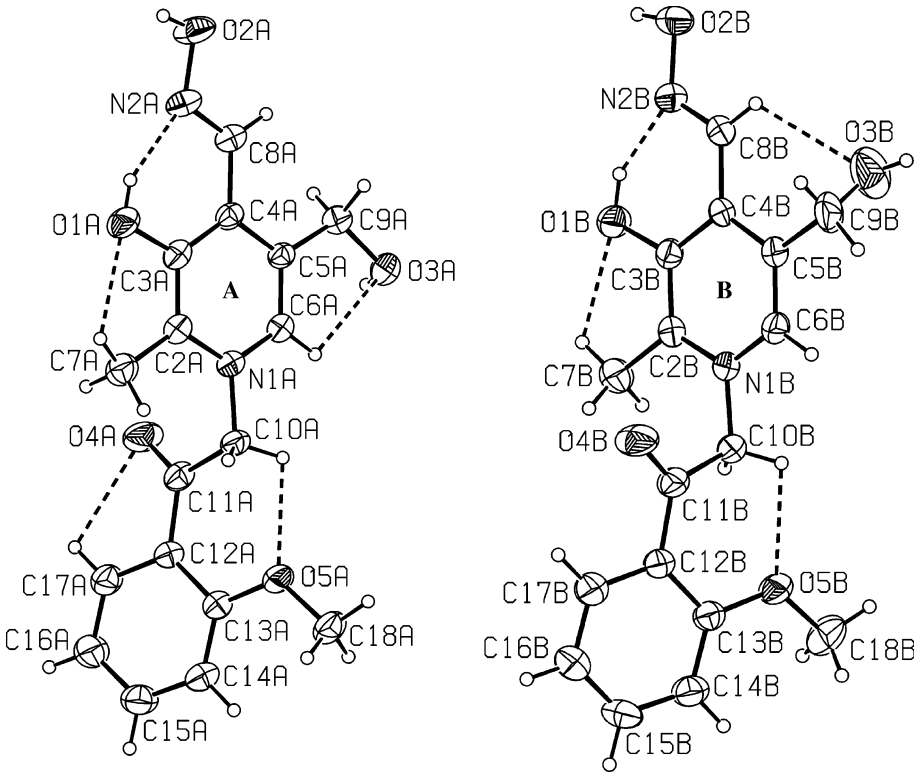

Fig. 2 The molecular structures of two independent cations of **3** (A and B), with the atom-numbering schemes. For clarity, only major component of disordered O3B atom is shown. Displacement ellipsoids for nonhydrogen atoms are drawn at the 30 % probability level. Intramolecular hydrogen bonds are shown dashed

Table 2 Hydrogen-bonding geometries of intramolecular hydrogen bonds in **2** and **3**

	D–H···A	D–H (Å)	H···A (Å)	D···A (Å)	D–H···A (°)
2	O1–H1···N2	0.73 (3)	1.91 (3)	2.561 (2)	149 (3)
	C6–H6···O3	0.93	2.35	2.727 (3)	104
	C7–H7B···O1	0.96	2.28	2.740 (3)	109
3	O1A–H1A···N2A	0.81 (2)	1.88 (2)	2.604 (3)	149 (3)
	C6A–H6A···O3A	0.93	2.31	2.710 (3)	105
	C7A–H72A···O1A	0.96	2.34	2.745 (3)	104
	C10A–H10B···O5A	0.97	2.30	2.658 (2)	101
	C17A–H17A···O4A	0.93	2.44	2.752 (3)	100
	O1B–H1B···N2B	0.86 (2)	1.78 (2)	2.551 (3)	148 (2)
	C7B–H72B···O1B	0.96	2.29	2.751 (3)	109
	C8B–H8B···O3B	0.93	2.47	2.981 (5)	115
	C10B–H10C···O5B	0.97	2.27	2.621 (3)	100

the pyridinium ring [C6B–C5B–C9B–O3B = 119.2(3)°], and it participates as acceptor in the C8B···O3B intramolecular hydrogen bond (Table 2).

From Figs. 1 and 2 is obvious that phenacyl moiety has different orientation in **2** and two independent cations of **3**. The conformation in two cations of methoxy derivative **3** is locked by the same, C10···O5, intramolecular hydrogen bond. Furthermore, phenacyl moiety in **2** and B cation of **3** is positioned in front of the pyridinium ring plane defined by the C2–N1–C10–C11 torsion angle of −87.8(2) and −77.3(2)° in **2** and B cation of **3,** respectively. The same torsion angle in A cation of **3** amounts 75.5(2)°, which means that phenacyl ring is at the opposite side of the pyridinium ring plane. Finally, there is one more intramolecular hydrogen bond in A cation of **3**, C17A···O4A, formed between phenyl ring hydrogen atom and carbonyl oxygen atom. This hydrogen bond is missing in **2** and B cation of **3**, because of slightly different phenyl ring orientation towards carbonyl group which is accompanied with longer H···O distance and smaller C − H···O angle.

Table 3 Hydrogen-bonding geometries of intermolecular hydrogen bonds in **2** and **3**

	D–H···A	D–H (Å)	H···A (Å)	D···A (Å)	D–H···A (°)	Symmetry codes
2	O2–H2···Br1	0.73 (3)	2.42 (3)	3.146 (2)	175 (3)	x, 3/2 − y, − 1/2 + z
	O3–H3···Br1	0.82	2.47	3.272 (2)	166	x, − 1 + y, z
	C10–H10A···Br1	0.97	2.88	3.726 (3)	146	−x, − 1/2 + y, 1/2 − z
	C6–H6···O2	0.93	2.43	3.259 (3)	149	x, 1/2 − y, 1/2 + z
	C13–H13···O3	0.93	2.38	3.301 (3)	171	−x, 1/2 + y, 1/2 − z
	C17–H17···O1	0.93	2.46	3.217 (4)	138	1 − x, − 1/2 + y, 1/2 − z
3	O2A–H2A···Br2	0.77 (3)	2.39 (3)	3.154 (2)	168 (3)	−x, 1 − y, 1 − z
	O3A–H3A···Br1	0.83 (2)	2.41 (2)	3.232 (2)	175 (2)	x, − 1 + y, 1 + z
	C10A–H10A···Br2	0.97	2.90	3.767 (2)	149	x, y, 1 + z
	C14A–H14A···Br1	0.93	2.83	3.701 (2)	157	−x, 1 − y, 2 − z
	C9A–H92A···O4B	0.97	2.56	3.436 (3)	150	1 + x, y, z
	O2B–H2B···Br2	0.83 (3)	2.34 (3)	3.166 (2)	173 (3)	−1 + x, y, 1 + z
	O3B–H3B···Br1	0.82	2.49	3.274 (5)	161	x, − 1 + y, 1 + z
	C6B–H6B···Br1	0.93	2.87	3.702 (2)	149	−x, 1 − y, 1 − z
	C8B–H8B···O4A	0.93	2.55	3.186 (3)	126	
	C9A–H92A···Cg1[a]	0.97	2.92	3.634 (3)	131	1 + x, y, z

[a] Cg1 is centroid of N1B–C6B ring

It can be predicted that such differences in conformation are caused by intermolecular interactions, especially hydrogen bonds in **2** and **3** (Table 3). E.g., conformation of hydroxymethyl group in two closely related structures [16] also differ. The C6–C5–C9–O3 torsion angle amounts 7.4(5)° in structure of pyridinium iodide derivative, the angle value being almost identical as those in **2** and A cation of **3**, and 119.52(15)° in structure of pyridinium chloride monohydrate, which is almost identical to the value of angle in B cation of **3**. The difference in conformation of the hydroxylmethyl group in similar structures is easy to explain as pyridinium chloride derivative is

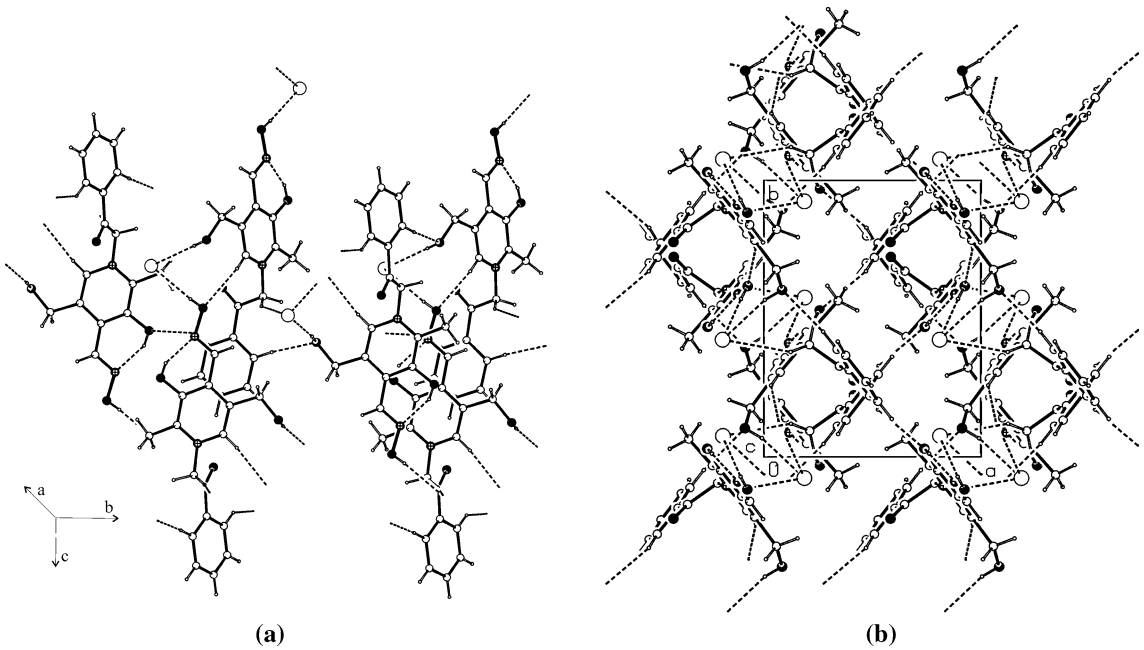

Fig. 3 **a** Part of the crystal structure of **2**, showing O−H···Br, C−H···Br and C−H···O hydrogen bonds; **b** A crystal packing diagram of **2**, viewed along the *c* axis. Hydrogen bonds are indicated by dashed lines

monohydrate and hydroxyl oxygen atom of the hydroxymethyl group points to the oxygen atom of water molecule.

A pyridoxal oxime cation and bromide ions in **2** are linked by two O–H···Br hydrogen bonds, O2···Br1 and O3···Br1, so forming finite pattern (Fig. 3a). The C10···Br1 hydrogen bond participates also in cation/anion connection. The cations are further link by three C–H···O hydrogen bonds, all of them forming different types of chains. The C6···O2 hydrogen bond generates *C*(7) [18] chains parallel to the *c* axis. Other two C–H···O hydrogen bonds, in which phenyl ring hydrogen atoms participate, C13···O3 and C17···O1, form *C*(10) and *C*(9) spirals parallel to the *b* axis. All this ensemble of hydrogen bonds forms three-dimensional network (Fig. 3b). On the crystal packing diagram along the *c* axis one can see very small channels (Fig. 3b). Some of them are partially occupied by bromides (at $x \approx 1/4$ and $x \approx 3/4$), but those at $x \approx 1/2$ are not occupied at all. It should be also mentioned that the pyridinium and phenyl rings do not participate in C–H···π and π···π stacking interactions.

The supramolecular assembling of **3** is completely different. There are only two C–H···O hydrogen bonds that mutually link A and B cations of **3**. The cations and bromides are linked by four O–H···Br hydrogen bonds in which O2 and O3 atoms participate as protondonors in both independent cations. Both bromides, Br1 and Br2, interconnect two independent cations, thus forming huge ring consists of four cations and four anions (Fig. 4a; indicated by ellipse). Thus, different conformation of the hydroxymethyl group in B cation could be a consequence of the O3B···Br1 hydrogen bond, as such orientation is necessary for ring formation. Bromide ions participate also in cations connection by three C–H···Br hydrogen bonds (Table 3). All hydrogen bonds in **3** form finite pattern, whereas C–H···O hydrogen bonds in **2** form infinite chains.

One C–H···π interaction between carbon atom of hydroxymethyl group and pyridinium ring of B cation participates also in supramolecular aggregation (Table 3). Finally, supramolecular structure of **3** contains also two weak aromatic π···π stacking interactions [19], the first one being between phenyl rings of the B cations. An interplanar angle between the rings is 0°, interplanar spacing is ca 3.75 Å, a centroid separation $4.1971(16)^{i}$ Å, and corresponding centroid–centroid offset ca 1.88 Å [symmetry code: (*i*) − 1−x, 1 − y, 1 − z]. Second aromatic π···π stacking interaction is accomplished between phenyl rings of two different independent cations, B and A. In this interaction, an interplanar angle between the rings amounts $8.84(13)^{\circ}$, interplanar spacings are ca 3.83 and 3.72 Å, respectively, a centroid separation $3.9660(16)^{ii}$ Å, and corresponding centroid–centroid offset ca 1.37 Å [symmetry code: (*ii*) x, y, − 1 + z]. π···π stacking interactions

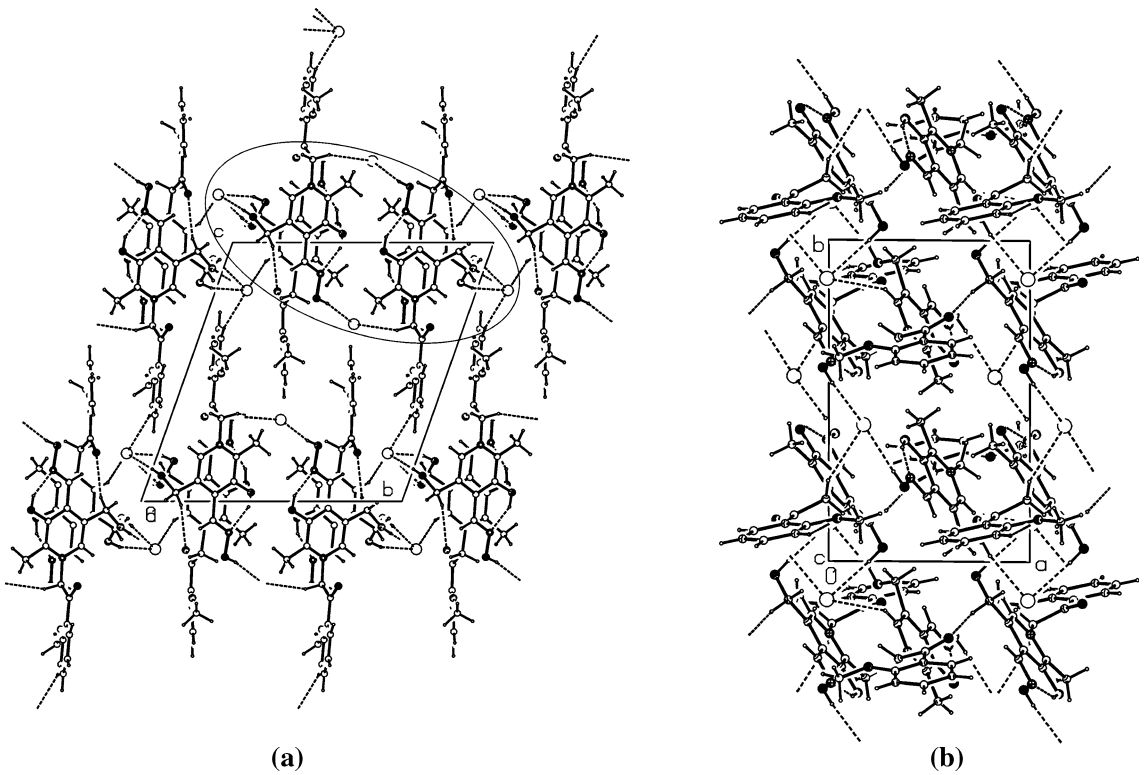

Fig. 4 **a** A crystal packing diagram of **3**, viewed along the *a* axis. The ellipse shows a ring formed by four O−H···Br hydrogen bonds; **b** A crystal packing diagram of **3**, viewed along the *c* axis. Hydrogen bonds are indicated by dashed lines

link four by four cations along the *b* axis in a *zig-zag* finite chains approximately at c = 1/2 (Fig. 4a). These C−H···π and π···π interactions completes three-dimensional network (Fig. 4b).

To conclude, a lot of intramolecular hydrogen bonds lock the conformation of these two pyridoxal oxime phenacyl derivatives. In derivative **3** that has methoxy group attached to phenyl ring, besides O–H···Br, C–H···Br and C–H···O hydrogen bonds, cations are additionally linked by C–H···π and π···π interactions. We believe that O–H···Br hydrogen bonds that form ring of four cations and anions, and π···π interactions which are lacking in **1**, are responsible for the different orientation of phenacyl moiety and conformation of this structure. In compound **2**, phenyl ring is included in intermolecular interactions exclusively through C–H···O hydrogen bonds. Thus, the conformation of these molecules is defined by discrete interplay between intramolecular and intermolecular interactions during the process of crystallization.

References

1. Somani SM, Romano JA Jr (2001) Chemical warfare agents: toxicity at low levels. CRS Press LLC, Boca Raton
2. Bajgar J (2004) Adv Clin Chem 38:151–216
3. Dohnal V, Kuča K, Jun D (2005) J Appl Biomed 3:139–145
4. Kuča K, Bartošová L, Jun D, Patočka J, Cabal J, Kassa J, Kunešová G (2005) Biomed Papers 149:75–82
5. Kassa J (2002) Clin Toxicol 40:803–816
6. Jokanović M, Stojiljković MP (2006) Eur J Pharmacol 553:10–17
7. Kovarik Z, Čalić M, Šinko G, Bosak A, Berend S, Lucić Vrdoljak A, Radić B (2008) Chem Biol Interact 175:173–179
8. Kovarik Z, Čalić M, Bosak A, Šinko G, Jelić D (2008) Croat Chim Acta 81:47–57
9. Primožič I, Odžak R, Tomić S, Simeon-Rudolf V, Reiner E (2004) J Med Chem Def 2:1–30
10. Reiner E, Simeon-Rudolf V (2006) Arh Hig Rada Toksikol 57:171–179
11. Milatović D, Vorkapić-Furač J, Škrinjarić-Špoljarić M, Reiner E (1989) Acta Pharm Jugosl 39:281–287
12. Gašo-Sokač D, Katalinić M, Kovarik Z, Bušić V, Kovač S (2010) Chem Biol Interact 187:234–237
13. Oxford Diffraction, Xcalibur CCD System. *CrysAlis CCD* and *CrysAlis RED*. Oxford Diffraction Ltd, Abingdon, England
14. Sheldrick GM (2008) Acta Crystallogr A64:112–122
15. Spek AL (2008) J Appl Crystallogr 36:7–13
16. Jukić M, Hergold-Brundić A, Cetina M, Nagl A, Vorkapić-Furač J (2003) Struct Chem 14:597–604
17. Allen FH (2002) Acta Crystallogr B58:380–388
18. Bernstein J, Davis RE, Shimoni L, Chang NL (1995) Angew Chem Int Ed Engl 34:1555–1573
19. Hunter CA, Sanders JKM (1990) J Am Chem Soc 112: 5525–5534